RP Current Trends In Applied Sciences
Vol. 2, No. 2 (April – June 2023) pp. 30–33
e-ISSN: 2583-7486

RESEARCH PLATEAU PUBLISHERS

Cite this article: N. Singh, Synthesis of SnO_2 nanoparticles by sol-gel method and their characterization, *RP Cur. Tr. Appl. Sci.* **2** (2023) 30–33.

Original Research Article

Synthesis of SnO_2 nanoparticles by sol-gel method and their characterization

Navneet Singh*
Department of Physics, Rajiv Gandhi Government College for Women, Bhiwani – 127021, Haryana, India
*Corresponding author, E-mail: ndhanda16@gmail.com

ARTICLE HISTORY
Received: 4 Jan. 2023
Revised: 5 April 2023
Accepted: 6 April 2023
Published online: 8 April 2023

KEYWORDS
Bandgap; Metal oxide; Tin oxide; Nanocrystallites; Sol-gel.

ABSTRACT
The straightforward sol-gel method was successfully used to create nanocrystalline SnO_2 powder. The SnO_2 nano-powder was made from the obtained sol-gel after it had been cleaned and heated to 400°C. X-ray diffraction (XRD) technique was used to examine the structural characteristics of (SnO_2) nanocrystalline powder. By capturing the absorbance and transmittance spectra, Uv-Vis Spectroscopy was used to investigate the optical properties. The XRD pattern of the initially generated sample showed that SnO_2 nanocrystallites had formed a rutile structure. The SEM examination revealed a uniform distribution of relatively tiny grains throughout the scanned area. The Uv-Vis absorbance spectra also revealed a distinguishing peak of absorbance for SnO_2 at λ = 312 nm. From the graph of variation of $(\alpha h\nu)^2$ with $h\nu$, the energy band gap measurement for nanocrystalline SnO_2 thin film was performed. 3.78 eV is the calculated optical bandgap energy for SnO_2 thin films. According to the findings, the synthetic SnO2 film transmits light at a rate of 78% between 350 and 800 nanometers.

1. Introduction

The fascinating features of semiconductor metal oxide nano-crystals, which differ from those of their corresponding bulk state, have generated a considerable deal of curiosity. Due to its many beneficial properties, including its wide band gap (E_g = 3.64 eV, 330 K), n-type conductivity, and high transparency in the visible range (> 80%), tin oxide (SnO_2) is one of the important metal oxides. It can be produced in a variety of shapes and sizes using various low-cost synthesis techniques, making it applicable for a variety of applications such as solid-state gas sensors, flat panel displays, and solar energy cells [1, 2]. The presence of excess interstitial tin, oxygen vacancies, and unintentional chlorine doping (primarily from glass substrates at higher deposition or calcination temperatures due to softening of soda lime glass) are the main causes of the high free carrier density in the thin films of SnO_2 that ranges from 10^{19} to 10^{20} cm^{-3}.

SnO_2 nanostructures with improved control over particle size and physical properties have been created using a number of innovative and successful techniques. These include the hydrothermal technique [3, 4], polymeric method [5, 6], synthesising organometallic precursors [6, 7], sonication method [8, 9], microwave method [9, 10], and surfactant-mediated method [11]. However, they are either time-consuming, expensive, and/or difficult. The hydrothermal process requires at least 24 hours to produce SnO_2 nanoparticles. Additionally, the polymeric and sonication processes are difficult to use and provide low throughputs, making them unsuitable for large manufacturing. Sol-gel, on the other hand, is a straightforward method for producing homogenous nanoparticles with high purity and crystallinity at a low temperature. Sol-gel processes convert a precursor solution into an inorganic solid by (a) dispersing colloidal particles in a liquid (sol) and (b) converting the sol into a rigid phase (gel) through hydrolysis and condensation reactions [12]. In most cases, it results in the formation of amorphous precipitates, and heat treatment is required to drive particle growth by re-crystallization and to change the particle shape. However, the sol gel approach is superior to alternative synthesis techniques for producing tin oxide due to its lower processing temperature, improved homogeneity and regulated stoichiometry, and flexibility in producing dense monoliths, thin films, and nanoparticles.

In the current study, we looked at the structural, morphological, and optical characteristics of SnO_2 nanopowder and thin films made using the quick and easy sol-gel method. With the help of several characterisation methods like X-ray diffraction (XRD), scanning electron microscopy (SEM), and UV-VIS spectroscopy, the characteristics of these SnO2 nanocrystallites have been investigated.

2. Experimental

2.1 Materials

Without additional purification, SnO_2 nanoparticles were created using Analytical Reagent (A.R.) grade chemicals including tin tetrachloride pentahydrate ($SnCl_4.5H_2O$), ethylene glycol, and ammonia (Make: Loba Chemie Pvt. Ltd. Mumbai, India). During the synthesis, precursors included $SnCl_4.5H_2O$, ethylene glycol, and liquid ammonia were dissolved in double-distilled water.

2.2 Method

Tin oxide nano-powder was created using the sol-gel process. In a beaker, 50 ml of double-distilled water was dissolved in the 0.1 molar of tin-tetrachloride pentahydrate (3.51 g of $SnCl_4.5H_2O$), and 50 ml of ethylene glycol was then added to create a 100 ml precursor mixture. The resulting

precursor mixture was stirred at 300 RPM using a magnetic stirrer (Make: Remi), and 0.1M of an aqueous ammonia solution was dropped into the mixture at a rate of 10 drops per minute while it was being stirred. About 50 drops of aqueous ammonia were added, and within 5 minutes the sol-gel had formed. To eliminate excess ammonia, the resultant gel was filtered using Whatman filter paper (grade-42) and then washed three to four times with double-distilled water. The material on the filter paper was then carefully deposited in a crucible and onto a glass substrate using a commercial applicator with a 1 m tip to create a thin layer. To get rid of the water molecules, the precipitate in the crucible and a thin layer were dried at 150°C for two hours. After drying, a film on glass substrate was coated with dark brown coloured tin oxide nano-powder, which was then further calcinated at 400°C for two hours. [13]. Figure 1 depicts the photographic illustration of the many steps involved in the sol-gel method's production of SnO_2 nanocrystallites.

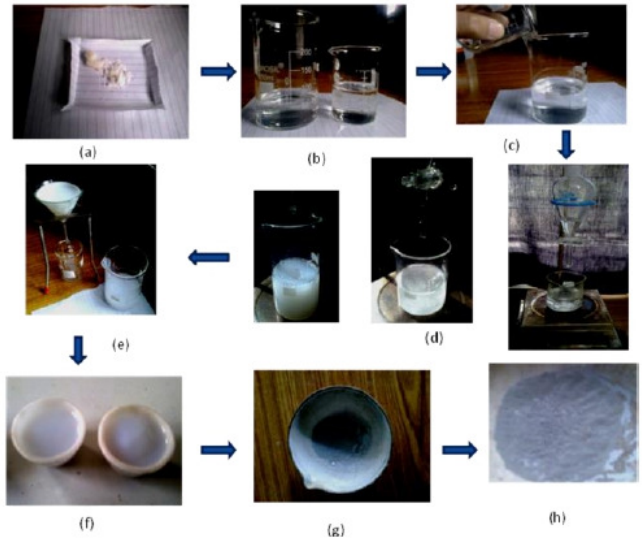

Figure 1: Stepwise photographic illustration of synthesis process of SnO_2 nanocrystallites. (*a*) precursor, $SnCl_4.5H_2O$, (*b*) solutions in beakers contain from left to right $SnCl_4.5H_2O$, ethylene glycol, (*c*) simultaneous addition, (*d*) gel formed by drop-wise addition aqueous ammonia under constant magnetic stirring, (*e*) filtration and washing, (*f*) gel of SnO_2 nanocrystallites, (*g*) dried SnO_2 nanocrystallites at 150ºC for 2 hrs. and (*h*) calcinated at 400ºC to obtain SnO_2 nanocrystallites in powder form.

2.3 Characterization

The structural properties of SnO_2 nano-powder were studied by X-ray diffraction measurements (Bruker D-8 advance diffractometer, Billerica, MA) using the Cu Kα (λ = 1.5406 Å) as a radiation source, operated at 40kV and 30 mA with a scan rate of 0.02°/s over the range of 10°-80°. The average crystallite size *d*(*hkl*) of all crystal planes for SnO2 powder was estimated from the classical Scherrer formula [14]:

$$D = \frac{K\lambda}{\beta \cos\theta}, \qquad (1)$$

where *K* is the shape factor usually has a value 0.9, λ is the X-ray wavelength and θ the Bragg angle and β gives the full width of the half maxima (FWHM).

The surface morphology of the SnO_2 powder was studied by scanning electron microscope (SEM). The spectral transmittance and absorbance measurements were obtained using UV-VIS spectrometer (Shimatzu 1650PC) in the spectral range of 250 nm to 800 nm. The X-intercept obtained by extrapolating the linear portion of the exponential curve from of the graph of $(\alpha h\nu^2)$ versus photon energy ($h\nu$) is the bandgap energy of the material.

3. Results and discussion

3.1 Structural and morphological properties

The powder X-ray diffraction analysis of the SnO_2 sample was performed in order to identify the phase, crystal structure and to estimate average grain size. The as recorded X-ray diffraction pattern of SnO_2 powder sample by sol-gel technique is as presented in Figure 2.

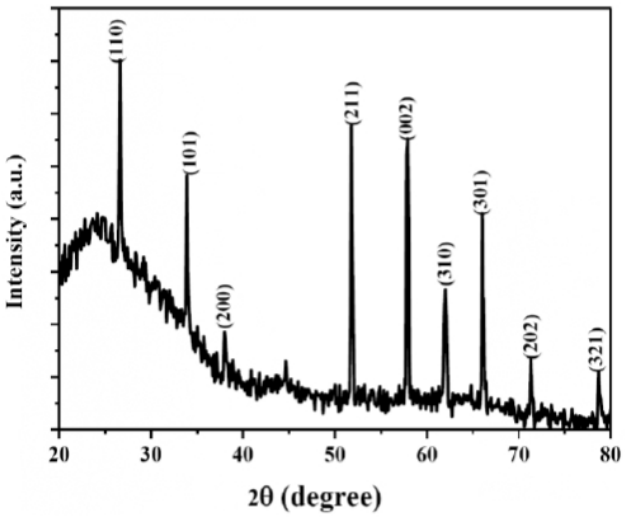

Figure 2: XRD pattern of SnO_2 nanocrystallites.

Table 1: XRD analysis of SnO_2 nanocrystallites

2θ	(*hkl*) planes	Inter-planar distances (*d*) (nm)
26.6°	(110)	58.9
33.9°	(101)	55.3
38.0°	(200)	43.6
51.8°	(211)	59.3
57.9°	(002)	57.7
62.0°	(310)	49.3
66.0°	(301)	51.7
71.3°	(202)	47.5
78.7°	(321)	44.4

The XRD pattern reveals the formation of SnO_2 nanoparticles with polycrystalline phase demonstrating rutile structure [JCPDS Card No: 41-1445, a = 3.1859 Å, c = 4.743Å]. The crystal planes (110), (101), (211), (002), (310), (301) were prominently seen in XRD indicating the polycrystalline nature of powder. The average value of lattice constant from different (*hkl*) planes was determined by using the formula, $a = d(h^2 + k^2 + l^2)^{1/2}$, where d is inter-planer distance and (*hkl*) are Miller indices. The calculated average values of lattice constant a = 3.1854 Å, c = 4.7470 Å. No impurity phase was observed. The average crystallite size (D)

as determined from the XRD spectra using Scherer's formula was 52 nm. The respective angles of peak positions (2θ), *hkl* planes and inter-planar distance (*d*) are represented in Table 1.

To determine the sample's morphological characteristics, SEM analysis was done. Figure 3 displays a SEM image of a thin sheet of nanocrystalline SnO_2. Figure 3 depicts the distribution of SnO_2 nanocrystallites throughout a scanned region as being homogeneous and uniform.

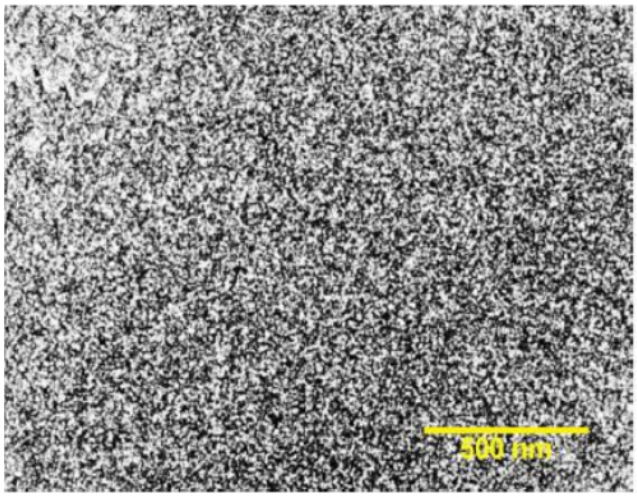

Figure 3: SEM micrograph of SnO_2 nanocrystallites.

3.2 Optical properties

The UV-VIS absorbance spectra of SnO_2 nanocrystallites are as represented in the Figure 4 and Figure 5 respectively. The characteristic absorption peak was found around 312 nm in the region (275 nm ≤ λ ≤ 350 nm). The substantial decrease in transmittance for SnO_2 nanocrystallites near the band edge indicates the better crystallinity and lower defect density for synthesized thin film. The SnO_2 thin film showed the transmittance of 78% in the spectral range of 350 nm – 800 nm.

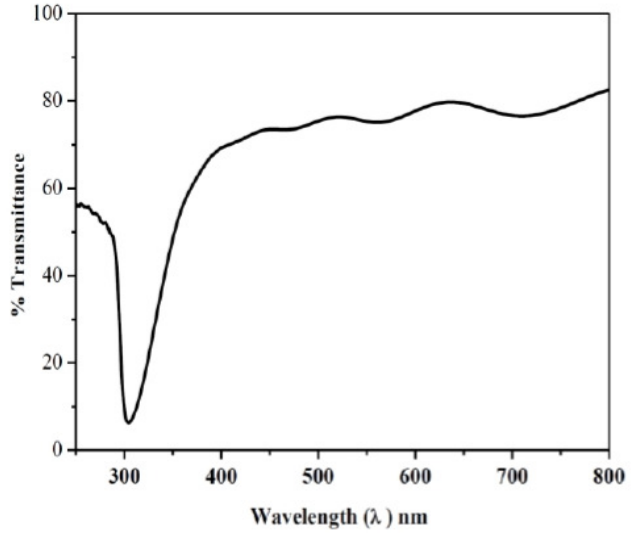

Figure 4: Transmittance spectrum of SnO_2 thin film.

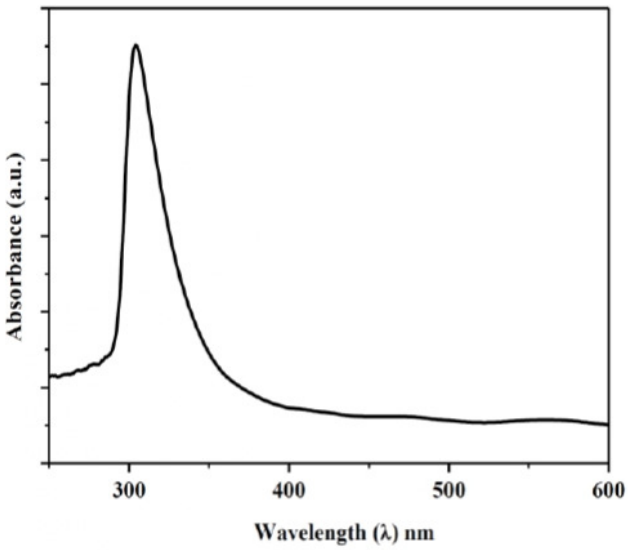

Figure 5: UV-VIS absorption spectrum of SnO_2 nanocrystallites.

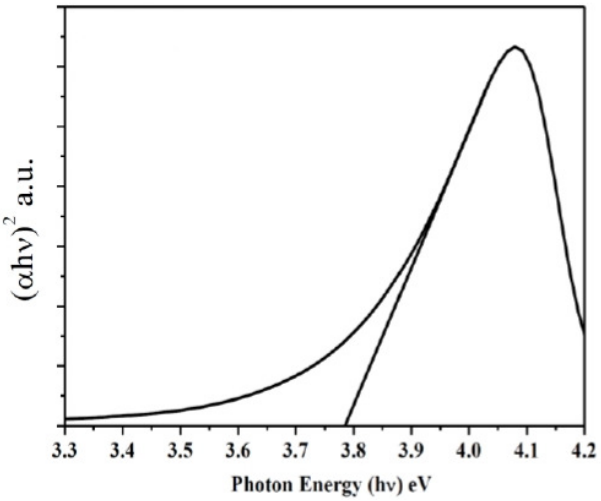

Figure 6: The plot of $(\alpha h\nu)^2$ vs $h\nu$ for SnO_2 nanocrystallites.

The analysis of the transmission Figure 4 (thin film) and absorbance spectra (absorbance for SnO_2 nanocrystallites) in the vicinity of the fundamental absorption edge shows that the variation of the absorption coefficient is in accordance with following relation which implies the direct transitions [15].

$$(\alpha h\nu)^2 = A(h\nu - E_g)\,. \qquad (2)$$

Here α is an absorption coefficient, *h* is Planck constant, ν is the frequency and $h\nu$ is the incident photon energy. Figure 6 represents the plot of $(\alpha h\nu)^2$ vs $h\nu$ for SnO_2 nanocrystallites.

The direct band gap (E_g) of our sample was measured from the absorption coefficient data as a function of wavelength using Tauc relation thereby extrapolating the straight line of the $(\alpha h\nu)^2$ vs. $h\nu$ plot to intercept on the horizontal photon energy axis and was found to 3.78 eV as shown in Figure 6. The produced tin oxide clearly exhibits a higher optical band gap than the value of 3.64 eV for bulk SnO_2 [16], which can be attributed to the quantum confinement effect.

4. Conclusions

The Sol-Gel process was used to successfully create thin films and nanocrystallites of tin oxide (SnO2). XRD examination has led us to the conclusion that the particles in question are polycrystallized with a tetragonal rutile structure. An SEM image of a thin layer of SnO_2 nanocrystallines reveals homogeneous dispersion of relatively small grains with an average crystallite size of 52 nm. The absorbance and transmittance spectra demonstrate that the homogeneous, smaller-sized tin oxide nanocrystallites produced using synthetic means. Uv-Vis analysis showed the characteristic absorbance peak at $\lambda = 312$ nm for SnO_2. The bandgap of SnO_2 nanocrystallites was measured from the plot of variation of $(\alpha h\nu)^2$ versus $h\nu$ was 3.78 eV. The transmittance analysis showed the transmittance of 78% for as synthesized SnO_2 thin film in the spectral range 350 nm to 800 nm.

References

[1] Z. Ying, Q. Wan, Z. Song, S. Feng, SnO_2 nanowhiskers and their ethanol sensing characteristics, *Nanotechnology* **15** (2004) 1682.

[2] A. Singh, U. Nakate, Microwave synthesis, characterization and photocatalytic properties of SnO_2, *Adv. Nanoparticles* **2** (2013) 66-70.

[3] H. Chiu, C. Yeh, Hydrothermal synthesis of SnO_2 nanoparticles and their gas-sensing of alcohol, *J. Phys. Chem. C* **111** (2007) 7256-7259.

[4] A. Firooz, A. Mahjoub, A. Khodadadib, Preparation of SnO_2 nanoparticles and nanorods by using a hydrothermal method at low temperature, *Mater. Lett*. **62** (2008) 1789-1792.

[5] E. Leite, I. Weber, E. Longo, J. Varela, A new method to control particle size and particle size distribution of SnO_2 nanoparticles for gas sensor applications, *Adv. Mater*. **12** (2000) 965-968.

[6] C. Nayral, E. Viala, P. Fau, F. Senocq, J. Jumas, A. Maisonnat, B. Chaudret, Synthesis of tin and tin oxide nanoparticles of low size dispersity for application in gas sensing, *Chem. Eur. J*. **6** (2000) 4082-4090.

[7] J. Zhu, Z. Lu, S. Aruna, D. Aurbach, A. Gedanken, Sonochemical synthesis of SnO_2 nanoparticles and their preliminary study as Li insertion electrodes, *Chem. Mater*. **12** (2000) 2557-2566.

[8] G. Pang, S. Chen, Y. Koltypin, A. Zaban, S. Feng, A. Gedanken, Controlling the particle size of calcined SnO_2 nanocrystals, *Nano Lett*. **1** (2001) 723-726.

[9] V. Subramanian, W. Burke, H. Zhu, B. Wei, Novel microwave synthesis of nanocrystalline SnO_2 and its electrochemical properties, *J. Phys. Chem. C* **112** (2008) 4550-4556.

[10] J. Jouhannaud, J. Rossignol, D. Stuerga, Rapid synthesis of tin (IV) oxide nanoparticles by microwave induced thermohydrolysis, *J. Solid State Chem*. **181** (2008) 1439-1444.

[11] Y. Wang, C. Ma, X. Sun, H. Li, Preparation and characterization of SnO_2 nanoparticles with a surfactant-mediated method, *Nanotechnology* **13** (2002) 565-570.

[12] P. Baker, R. Sanderson, A. Crouch, Sol–gel preparation and characterisation of mixed metal tin oxide thin films, *Thin Solid Films* **515** (2007) 6691-6697.

[13] S. Gnanam, V. Rajendran, Luminescence properties of EG assisted SnO_2 nanoparticles by sol-gel process, *Dig. J. Nanomater. Biostruct*. **5** (2010) 699-704.

[14] H. Klug, L. Alexander, X-Ray Diffraction Procedures: For Polycrystalline and Amorphous Materials, John Wiley and Sons, New York, USA (1974).

[15] R. Swarnkar, S. Singh, R. Gopal, Effect of aging on copper nanoparticles synthesized by pulsed laser ablation in water: structural and optical characterizations, *Bull. Mater. Sci*. **34** (2011) 1363-1369.

[16] A. Azam, S. Habib, N. Salah, F. Ahmed, Microwave-assisted synthesis of SnO_2 nanorods for oxygen gas sensing at room temperature, *Int. J. Nanomedicine* **8** (2013) 3875-3882.